Chemosphere 206 (2018) 203–216

Contents lists available at ScienceDirect

Chemosphere

journal homepage: www.elsevier.com/locate/chemosphere

Geospatial analysis of residential proximity to open-pit coal mining areas in relation to micronuclei frequency, particulate matter concentration, and elemental enrichment factors

Lyda Espitia-Pérez [a, b, *], Marcia Arteaga - Pertuz [a, c, **], José Salvador Soto [d], Pedro Espitia-Pérez [a], Shirley Salcedo-Arteaga [a], Karina Pastor–Sierra [a], Claudia Galeano–Páez [a], Hugo Brango [e], Juliana da Silva [f], João A.P. Henriques [b]

[a] *Facultad de Ciencias de la Salud, Laboratorio de Investigación Biomédica y Biología Molecular, Universidad del Sinú, Montería, Córdoba, Colombia*
[b] *Departamento de Biofísica, Instituto de Biociências, Universidade Federal do Rio Grande do Sul, Porto Alegre, RS, Brazil*
[c] *Instituto de Políticas Públicas e Relações Internacionais–IPPRI, Universidade Estadual Paulista Júlio de Mezquita Filho, São Paulo, Brazil*
[d] *Departamento de Geografía y Medio Ambiente, Universidad de Córdoba, Colombia*
[e] *Instituto de Matemática e Estatística, Universidade de São Paulo, São Paulo, Brazil*
[f] *Laboratório de Genética Toxicológica, Universidade Luterana do Brasil, ULBRA, Canoas, RS, Brazil*

HIGHLIGHTS

- MNMONO frequencies and PM_{10} levels were clustered at south of the coal mining area.
- Higher MN frequencies were found in the flat areas surrounded by small hilltops.
- Spatial correlations among MNBN/$PM_{2.5}$ were established in pits and disposal sites.
- Higher EF of S and Cr were more related to an increased frequency of MNMONO cells.
- Wind and topography in mining areas were major contributors to damage distribution.

GRAPHICAL ABSTRACT

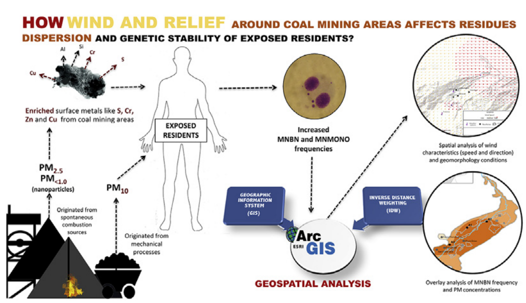

ARTICLE INFO

Article history:
Received 10 February 2018
Received in revised form
2 April 2018
Accepted 9 April 2018
Available online 3 May 2018

Handling Editor: R. Ebinghaus

Keywords:
Coal mining

ABSTRACT

During coal surface mining, several activities such as drilling, blasting, loading, and transport produce large quantities of particulate matter (PM) that is directly emitted into the atmosphere. Occupational exposure to this PM has been associated with an increase of DNA damage, but there is a scarcity of data examining the impact of these industrial operations in cytogenetic endpoints frequency and cancer risk of potentially exposed surrounding populations. In this study, we used a Geographic Information Systems (GIS) approach and Inverse Distance Weighting (IDW) methods to perform a spatial and statistical analysis to explore whether exposure to $PM_{2.5}$ and PM_{10} pollution, and additional factors, including the enrichment of the PM with inorganic elements, contribute to cytogenetic damage in residents living in proximity to an open-pit coal mining area. Results showed a spatial relationship between exposure to

* Corresponding author. Facultad de Ciencias de la Salud, Laboratorio de Investigación Biomédica y Biología Molecular, Universidad del Sinú, Calle 38 Cra. 1 W, Barrio Juan XXIII, Montería, Córdoba, Colombia.
** Corresponding author. Instituto de Políticas Públicas e Relações Internacionais – IPPRI, Universidade Estadual Paulista Júlio de Mezquita Filho, Praça da S;, 108–3º andar, São Paulo, Brazil.
E-mail addresses: lydaespitia@unisinu.edu.co (L. Espitia-Pérez), mapertuz@usp.br (M. Arteaga - Pertuz).

https://doi.org/10.1016/j.chemosphere.2018.04.049

IDW
GIS
Particulate matter
Micronuclei

elevated concentrations of $PM_{2.5}$, PM_{10} and micronuclei frequency in binucleated (MNBN) and mononucleated (MNMONO) cells. Active pits, disposal, and storage areas could be identified as the possible emission sources of combustion elements. Mining activities were also correlated with increased concentrations of highly enriched elements like S, Cu and Cr in the atmosphere, corroborating its role in the inorganic elements pollution around coal mines. Elements enriched in the $PM_{2.5}$ fraction contributed to increasing of MNBN but seems to be more related to increased MNMONO frequencies and DNA damage accumulated in vivo. The combined use of GIS and IDW methods could represent an important tool for monitoring potential cancer risk associated to dynamically distributed variables like the PM.

1. Introduction

Particulate matter (PM) generated during coal mining is described as PM_{10} (particles with aerodynamic diameters smaller than 10 μm), $PM_{2.5}$ (particles with diameters smaller than 2.5 μm) and $PM_{<1.0}$ (particles with diameters smaller than 1.0 μm), also called ultrafine particle fraction (UFP) (Agudelo-Castañeda et al., 2017). PM_{10} often referred to as the coarse fraction, is mostly produced by mechanical processes. By contrast, $PM_{2.5}$ is mainly derived from combustion sources, such as automobiles, trucks, and other vehicle exhaust, as well as from stationary combustion sources and $PM_{<1.0}$ is generated by photochemical processes and combustion, also from various natural and anthropogenic sources (Campagna et al., 2017). These elements incorporated with atmospheric PM may enter the body through inhalation (Li et al., 2015). PM_{10} is potentially hazardous to health, due to the complex composition of this fraction and easily mediated deposition in bronchi and lungs (Kaonga and Kgabi, 2011). The $PM_{2.5}$ fraction represents the highly-inhalable fraction of PM directly affecting the alveolar lung region (Barja et al., 2013).

Besides the size component, around coal mines, PM can contain high concentrations of toxic trace elements, such as dust particles (Ghose and Majee, 2007), Polycyclic Aromatic Hydrocarbons – PAHs (Pone et al., 2007; Ribeiro et al., 2010), and metals (Bhuiyan et al., 2010; Dubey et al., 2012; Espitia-Pérez et al., 2016). Particularly, metals are an important class of carcinogens (Tchounwou et al., 2012) related to open-pit coal mining activities (Bhuiyan et al., 2010; Dubey et al., 2012). In fact, one of the major sources of anthropogenic trace element inputs in the atmosphere is coal combustion (Melody and Johnston, 2015; Sun et al., 2016). In recent years, there is a growing concern regarding the potential contribution of ingested dust to metal toxicity in humans. Some trace metals (such as Cu and Zn) at small amounts are harmless, but some (mainly Pb, As, Hg, and Cd) even at extremely low concentrations are toxic and are potential cofactors, initiators or promoters in many diseases, including and cancer (Annangi et al., 2016). Several health-related studies indicate a strong association of airborne PM generated around coal mines with adverse impacts such as increased cardiovascular disease, pneumoconiosis, neurotoxic effects, and different types of cancer (Ahern and Hendryx, 2012; Hosgood et al., 2012; Jenkins et al., 2013; Patra et al., 2016). Evidence suggests that PM exerts its genotoxic and carcinogenic effects through the generation of DNA damage and chromosomal instability (Rohr et al., 2013; León-Mejía et al., 2014). The cytokinesis-block micronucleus cytome (CBMNCyt) assay is a powerful tool for measuring comprehensively chromosomal instability phenotype and altered cellular viability caused by exogenous genotoxins (Fenech, 2006). The micronuclei (MN) frequency in peripheral blood lymphocytes can be predictive of cancer risk, and an increased MN formation is associated with early events in carcinogenesis (Bonassi et al., 2007, 2011). In the CBMN-cyt assay, micronuclei are scored specifically in binucleated (MNBN) and mononucleated (MNMONO) cells. MNBN is a biomarker of chromosome breakage and/or whole chromosome loss and MNMONO a biomarker of chromosomal damage induced and expressed in vivo before the start of the CBMN assay culture (Fenech, 2007). MN frequencies in MONO cells may give an estimation of the genome instability accumulated over many years in stem cells and circulating T lymphocytes, thus before the blood was sampled, whereas MN frequencies in BN cells additionally provide a measure of the lesions that have accumulated in the DNA or key proteins (Kirsch-Volders et al., 2014). Several studies have used MN frequencies to assess the potential risk of populations exposed to coal mining residues at the workplace (Leon-Mejia et al., 2011; Klimkina, 2013; Rohr et al., 2013). However, there is a scarcity of data examining the impact of these industrial operations in potentially exposed surrounding populations.

The open pit coal-mining region of northern Colombia covers an area of 69.000 ha (ha) and includes a 150 Km railroad and a port facility in the Atlantic ocean (Cerrejón, 2011). Air quality systems established to monitor PM levels around the coal mining area, are located in zones under the direct influence of prevailing winds and are limited to the south of open-pits, roads, industrial activities and disposal sites within the mining concession (Calderon and Nieves, 2010). Thus, most inhabitants around the mining zone may live in unmonitored areas or monitor-sparse locations. In a recent study, we demonstrated elevated MNBN and MNMONO frequencies in populations living in proximity to coal mining operations of northern Colombia (Espitia-Perez et al., 2017). Statistical correlation analysis suggested a strong association between MN frequencies, PM concentrations and elemental composition (particularly with some enriched elements like Cr, Cu, Zn, and S). Considering that PM distribution may be related to geomorphological characteristics and wind conditions in sampled areas, this article constitutes an extension of our previous approach in two ways: *i)* variables are analyzed using several spatial interpolation and geostatistics methodologies usually not considered in common statistical analysis applied to exposure risk studies in human populations, and *ii)* the analysis of the spatial relationship between $PM_{2.5}$, PM_{10} concentrations, MNBN, MNMONO frequencies and Enrichment Factor (EF) values for the PM, allows the evaluation of the proximity effect of coal mining on MN frequencies and the identification of potential distribution patterns that can reveal a potential risk in unmonitored populations. Spatial interpolation is a method or mathematical function that estimates the values at locations where no measured values are available. This method assumes the attribute data are continuous over space and spatially dependent, indicating that values closer together are more likely to be similar than the values farther apart. The goal of spatial interpolation is to create a surface that is intended to best represent empirical reality thus the method selected must be assessed for accuracy (Azpurua and Ramos, 2010). Inverse Distance Weighting

(IDW), Ordinary Kriging (OK) and Radial Basis Functions (RBF) are three well-known spatial interpolation techniques commonly used for characterizing the spatial variability and interpolating between sampled points and generating the prediction maps (Zandi et al., 2011). IDW and its modifications are the most often applied deterministic interpolation method (Nalder and Wein, 1998). This technique is based on the assumption that nearby values contribute more to the interpolated values than distant observations. In other words, for this method, the influence of a known data point is inversely related to the distance from the unknown location that is being estimated. According to several authors, IDW method can be used as the first choice to predict PM concentrations in regions where not enough measurement data are available (Wu et al., 2006; Jha et al., 2011).

2. Methodology

2.1. Study area and sampling site location

The open pit coal-mining region object of the present study is located in the semiarid southern part of the Department of La Guajira in northeast Colombia between the municipalities of Albania, Barrancas, and Hatonuevo. It is composed of indigenous Wayúu settlements, a small Afro-Colombian population, and some campesino (rural peasant) communities. Other areas influenced by the coal mining process include those areas around the port facility in the municipality of Uribia on the Caribbean Sea, where the coal is exported. Sampling sites were located in the area of direct influence of the mining operations in five sampling zones around or in proximity to different mining operations activities and around the port facility (Media Luna). The study, focus on villages located in the flat area around the coal mining corridor where high levels of PM_{10} have been reported by local air quality network of the regional environmental agency (CORPOGUAJIRA). The unexposed (Control) area was located in Mayapo municipality, also constituted of indigenous Wayúu settlements and Afro-Colombian populations, situated on the Caribbean sea without any influence of coal mining operations and located 57.12 km from the city of Riohacha.

2.2. Human biomonitoring

Samples were collected from individuals with permanent residence in proximity to the open-pit coal mining area (exposed) and from the non-mining area (control). All participants lived in the same areas where PM monitoring was performed. Thus, permanent residence was defined as at least 18 uninterrupted years for both areas. Blood samples were collected and transported simultaneously to prevent any interference caused by differences in sampling conditions. The collection was performed on 139 healthy individuals: 98 with permanent residential proximity to open − pit coal mining area and 41 permanent residents of a control area without any proximity to open-pit coal mining facilities. Exposed and unexposed control individuals were matched by age (±5 years), sex, similar social-economic status, and ethnicity. Participants were instructed to respond to a detailed, standard questionnaire that included data on health status (use of prescription medicines), cancer history, other chronic diseases, lifestyle, nutrition, smoking habits, the frequency of alcohol consumption and previous exposure to medical X-rays. Exclusion criteria for exposed and non-exposed groups were age over 65 years or less than 18 years, smoking (current and ex-smoking habits), actual medical treatment or up to 3 months or X-ray up to 1 year before sampling, therapeutic drugs intake known to be mutagenic, previous occupational exposure to coal mining residues, no permanent residence in each studied area and exposure to other PM sources.

2.3. Cytokinesis-block micronucleus (CBMN) assay

CBMN assay was carried out according to previously described methodology (Espitia-Perez et al., 2017). Briefly, heparinized whole blood (0.5 mL) was added to 4.5 mL of RPMI 1640 medium (Sigma R8758, USA) supplemented with 2 mM l-glutamine (Sigma G-3126, USA), 10% fetal bovine serum (Gibco/Invitrogen 15000-044, Brazil), 100 μL/mL antibiotic-antimycotic (Sigma A5955, USA) and 2% phytohemagglutinin (Sigma L8754, USA). Cultures were incubated at 37 °C in the dark for 44 h, under 5% CO_2. 6 μg/mL of cytochalasin B (Sigma, C6762) was added at the 44th h of incubation. After incubation, lymphocytes were harvested via centrifugation at 1200 rpm for 8 min, re-centrifuged, fixed in 25:1 (v/v) methanol/acetic acid, placed on a clean microscope and stained with Diff-Quik stain (Lab-Aids; LP64851). For each blood sample, 2000 binucleated cells (BN) (i.e., 1000 from each of the two slides prepared from the duplicate cultures) were scored for the presence of MN (MNBN) using bright-field optical microscopy at a magnification of 200−1000×. Additionally, MN frequency in 1.000 mononucleated cells (MONO) was evaluated to determine MNMONO frequency (Espitia-Perez et al., 2017). All slides were scored by a trained reader blinded to the exposure status of the individuals. The scoring criteria followed those proposed by (Fenech, 2007).

2.4. Sampling of atmospheric particulate matter

Samples of atmospheric particulate matter were collected from each site concomitantly with the human biomonitoring. For $PM_{2.5}$ collection, a total of twenty-five aerosol samples were collected using 46.2 mm PTFE filters (Tisch Environmental Inc., Cincinnati, OH, USA) and a PQ200 FRM air sampler (BGI MesaLabs, Butler, NJ, USA) with a $PM_{2.5}/PM_{10}$ inlet and a WINS impactor. According to CFR 40 part 50, appendix L (EPA, 2006), the air sampler was used with an air flow rate of 16.7 L/min and was calibrated before its use, using a flow calibrator MesaLabs DryCal Definer 220. On-site calibrations included volumetric flow verification through the samplers via comparison of the calibrated orifice results to the volumetric flow controller tables. Filters were weighed using an electronic microbalance (Radwag MYA11-3Y) with a resolution of 10^{-6} g. PM_{10} data from monitoring sites around the coal mining area were kindly provided by CORPOGUAJIRA. All samples in coal mining and control areas were collected in residential spaces and under similar weather conditions between August and December of 2015. All samples in coal mining and control areas were collected in residential spaces and under similar weather conditions between August and December of 2015.

2.5. Elemental composition and enrichment factor (EF) analysis

Using data from element concentrations previously obtained by PIXE analysis, we performed an Enrichment Factor (EF) analysis to identify those elements with an anthropogenic source. For analysis, elements with $EF < 10$ were considered as non-enriched, $10 < EF < 100$ as moderately enriched and $EF > 100$ as highly enriched (Taner et al., 2013). For this study, Al and Na were used as reference elements for the crust and marine sources, respectively. Concentrations of elements in the upper continental crust were taken from Wedepohl (Hans Wedepohl, 1995).

2.6. Spatial analysis

To explore the relationship between the variables ($PM_{2.5}$, PM_{10}, MNBN, MNMONO and EF values), a statistical analysis was performed by the software package SPSS version 16.0. For the spatial visualization of the calculated data, a geo-statistical method was employed by using ArcGIS Software Version 10.3.1 (ESRI, Redlands, CA, USA) and previous data obtained during the sampling process for each variable (Espitia-Perez et al., 2017).

Direct influence area of the mining project, open-pits, and disposal sites was georeferenced from previous reports (Espitia-Perez et al., 2017). Sampling sites (Rancherias) and surrounding coal mining areas were digitalized as reference points and used as a base layer for variable processing, analysis and spatial representation during the whole study. The digitalized map shows currently active open-pits, which include: Comuneros Pit, Oreganal Pit and NAM (New Areas of Mining) Pits (actually open-pits composed by La Puente and Tabaco Pits) (Fig. S1).

Geographic information system (GIS) was used to spatially analyze the distribution, enrichment level, and induced MNBN and MNMONO frequencies of $PM_{2.5}$ and PM_{10} around the coal mining area. Interpolation layers of each of the variables were obtained by IDW. The IDW method was applied to map the spatial characteristics of pollutants based on the ArcGIS 10.3.1 software. IDW interpolation method was selected considering sampling sites density and topography conditions of the studied areas (Espitia-Perez et al., 2017) where coastal zones and areas with proximity to open-cast pits share almost exclusively a flat geomorphology, except south, when it becomes slightly undulated in the vicinity of Cerro de Hatonuevo, with the presence of small hilltops (Fig. 1).

IDW employs a specific number of nearest points that are then weighted according to their distance from the point being interpolated applying the algorithm:

$$z^j_{est} = \frac{\sum\left(\frac{Z_i}{(h_{ij}+s)^2}\right)}{\sum\left(\frac{1}{(h_{ij}+s)^2}\right)}$$

where z^j_{est}: estimated value for location.

j, Z_i: measured sample values at point i.

h_{ij}: distance between z^j_{est} and Z_i.

S: smoothing factor (0).

2.6.1. Overlay analysis

Spatial relationships between the different data sets were studied creating new layers from the joint analysis of MN frequencies, $PM_{2.5}$, PM_{10} and EF values by using the Spatial Analysis Tool (Map Algebra) in ArcGIS. To enable the quantitative comparison of the different maps, they were all produced at the same spatial scale and on the same grid. Maximum and minimum values of the contour intervals obtained for each parameter inside the coal mining area were used to establish a three-rank categorization for MNBN, MNMONO, $PM_{2.5}$, PM_{10} values (high, medium and low) and a five-rank categorization for the EF values (very high, high, medium, low and very low). Range values and rank categorization are presented in Fig. S2A. Using the raster summation function of Map Algebra, this numerical treatment was used for the re-classification of the numerical values in three qualitative classes for MNBN/$PM_{2.5}$ and MNMONO/PM_{10} and five qualitative classes for MNBN/MNMONO/EF creating another layer of summed pixels (Fig. S2B). Using these numerical values, we obtained output raster overlay maps for MNBN/MNMONO frequencies and $PM_{2.5}$/PM_{10} levels and MNBN/MNMONO frequencies and EF values input rasters. Intervals were represented using a color scale, where lower values were represented by light colors and higher values using red.

3. Results

Detailed demographic characteristics of the studied population are described in Table 1. The mean age of the exposed group was 35.20 ± 13.34 years (range, 18–62 years), and of the non-exposed control group was 30.69 ± 11.56 years (range, 18–57 years). No significant difference in average age, social-economic status or dietary habits between exposed and unexposed individuals were detected. Analysis of MNBN and MNMONO frequencies in the total population (Table S1) revealed a significant increase in both parameters in individuals with residential proximity to the open pit coal mine compared to residents of the control area without proximity to coal mining facilities.

To identify possible emission sources at the sampling sites, all maps figures show spatial location of pits, disposal, and storing areas inside the mining areas. Coal storage piles (A1, A2, and A3) were identified from a previous report (Rojano et al., 2016). A1 and A2 are located in the north of the mining zone. A1 consisted in 11 storing piles at the north of the main area, and A2 is formed by 1 storing pile. A3 was located in the southern area of the mine, with a total number or 2 auxiliary piles for storing.

Spatial analysis of wind characteristics (speed and direction) and geomorphology conditions in sampling areas in proximity to the open pit coal mining operations is shown in Fig. 1.

Fig. 2 represents the spatial relation between MNBN frequencies and $PM_{2.5}$ concentrations around the coal mining area. Geographical distribution of both variables confirmed previous observations about the high correlation between MNBN and $PM_{2.5}$ concentrations. Higher spatial correlations between these variables were established for Chancletas, Provincial and San Francisco, located between disposal areas and active pits. A medium correlation was observed around the north and south of the mining area.

Interestingly, even when in previous reports MNMONO frequencies showed no correlation with PM_{10} concentrations (Espitia-Perez et al., 2017), the geographical distribution showed a high positive correlation of both variables at the south of the mining area (Fig. 3). A medium to low correlation was observed around rehabilitated pits and disposal sites located north of the mining area, where lower values of both variables were registered.

Based on the EF values of the studied elements and using the IDW interpolation method, their spatial distribution maps are shown in Fig. 4. Elements typically found around coal mining areas like S, Cu and Zn showed highly enriched patterns around areas with proximity to pits and disposal sites, with a decrease of enrichment factor with distance from the mining operations. Sulfur was highly enriched around the whole mining area, showing higher values around Chancletas, Provincial and San Francisco, while Cerro de Hatonuevo and Media Luna showed lower levels of S but higher concentrations of Cl and Cr. Analysis of the enrichment pattern for Cr also showed higher values at north and south of the mining region, particularly around pits and disposal sites. Similarly, Cl showed a poor enrichment pattern around the coal mining area and higher values at the north of the influence zone.

Spatial correlation between MNBN and MNMONO frequencies and enriched elements in mining areas are shown in Figs. 5 and 6 respectively. Compared to MNBN frequencies, MNMONO were more correlated to the EF values of S, Cr, and Cl. Instead, MNBN/MONO showed no spatial correlation with Zn enrichment values. Areas with enriched values of Cu were proportionately correlated with MNBN and MNMONO frequencies.

4. Discussion

Even when $PM_{2.5}$ fraction represents a high-risk for human health (Huang et al., 2017), $PM_{2.5}$ assessment has rarely been taken into account in biomonitoring studies. In fact, the Colombian legislation has only recently established national standards for $PM_{2.5}$ levels, thus previously $PM_{2.5}$ levels were not regularly

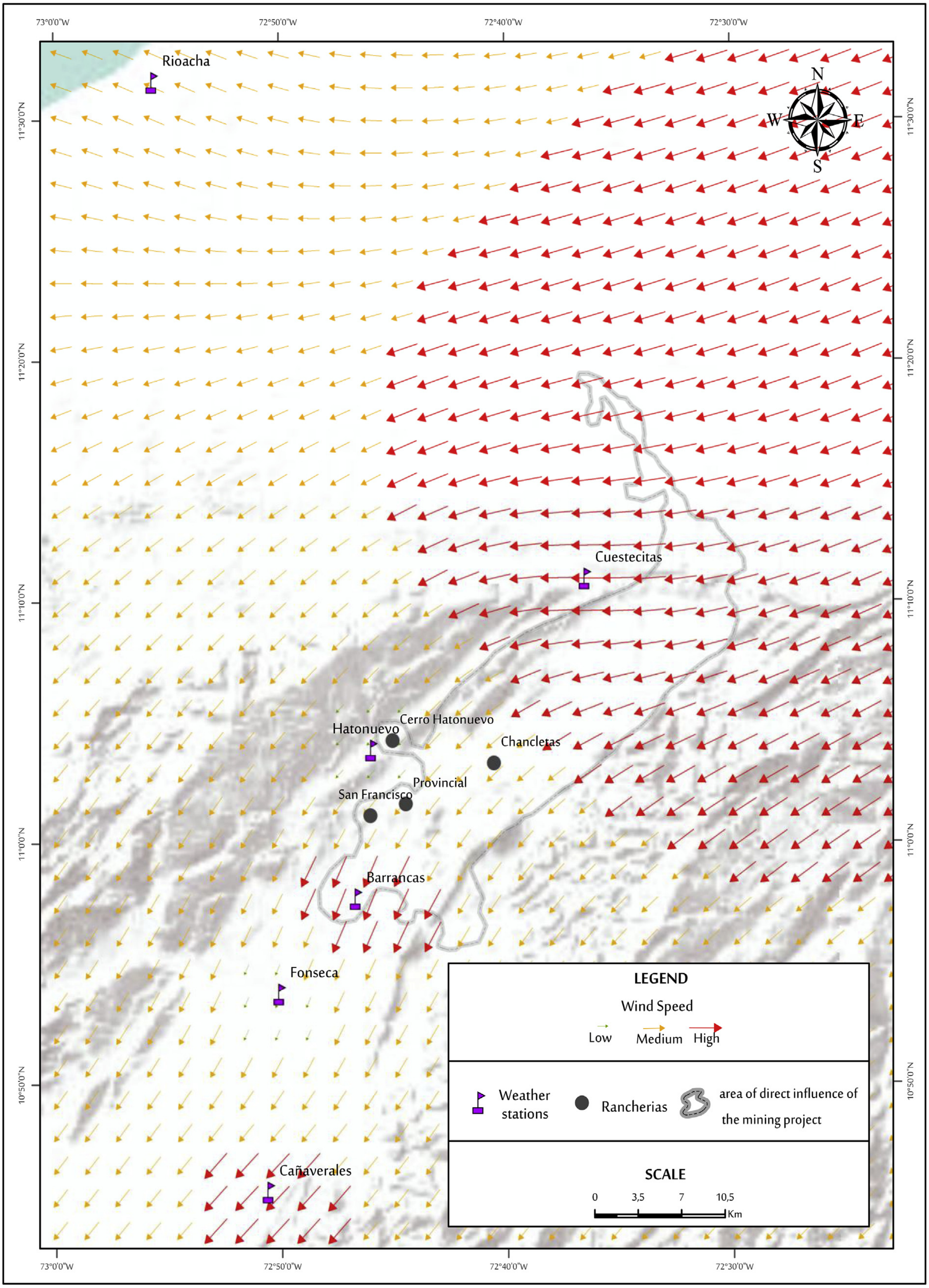

Fig. 1. Spatial analysis of wind characteristics (Speed and direction) and geomorphology conditions in sampling areas in proximity to the open pit coal mining operations.

Table 1
Main demographic characteristics of the studied population: exposed residents and control individuals.

Demographic characteristics	Group	
	Unexposed controls (Mean ± SD)	Exposed residents (Mean ± SD)
Number of individuals	41	98
Individuals by area		
Mayapo (Reference area/unexposed)	41	–
Provincial	–	20
San Francisco	–	26
Chancletas	–	21
Cerro de Hatonuevo	–	16
Media Luna	–	15
Gender n (%)		
Women	30 (73.17%)	68 (69.38%)
Men	11 (26.82%)	30 (30.61%)
Age (mean ± S.D)[a]	30.69 ± 11.56	35.20 ± 13.34

S. D: Standard deviation.
[a] Considered also as the time of exposure in the exposed resident's populations.

monitored (Ministerio del Ambiente, 2017). During the sampling period, $PM_{2.5}$ around the coal mining corridor showed a mean value of 22.80 ± 10.74 μg/m^3 with concentrations ranged from 7.02 to 39.39 μg/m^3. Most $PM_{2.5}$ levels in Chancletas and some $PM_{2.5}$ levels obtained for Provincial exceeded the 24-h fine particle standard established by the WHO (25 μg/m^3) and by the new Colombian legislation (37 μg/m^3). In contrast, PM_{10} levels showed a mean value of 43.09 ± 11.01 μg/m^3, well below new national air quality standards for 24 h (75 μg/m^3) (Ministerio del Ambiente, 2017) but with some values surpassing the particle standard established by the WHO (50 μg/m^3) for the same period. However, because our objective was to record actual exposure levels experienced by local residents and do not intend to evaluate regional air quality, this information was mainly used for informative means. Compared to previously reported values of PM_{10} in proximity to open-pit coal mines of England and the Czech Republic, our measures were significantly higher (Table S2). Interestingly, our values also surpassed previous reports for PM_{10} around the same coal mining area (Rojano et al., 2015). On the other hand, as also shown in Table S2 the few previously reported data on $PM_{2.5}$ concentrations are higher than our findings.

Results from the spatial analysis performed to MNBN frequencies and $PM_{2.5}$ concentrations using the IDW interpolation confirmed our previous observations about the high correlation between MNBN and $PM_{2.5}$. Higher spatial correlations between these variables were established for Chancletas, Provincial and San Francisco, located between disposal areas and active pits, where spontaneous coal seams fires are more common (Colaizzi, 2004). These spontaneous fires could be the main source of $PM_{2.5}$ around these areas if we consider that about 97% of $PM_{2.5}$ around coal mining facilities is produced in the combustion of coal (Cao Guo Liang et al., 2011). As shown in Fig. 2, exposure to $PM_{2.5}$, as well as MNBN frequency tends to decrease as the distance from the emission source increases, as evidenced in distant and elevated areas like Cerro de Hatonuevo. Despite being located in the proximity to coal mining operations and inside the direct influence of the mining area, Cerro de Hatonuevo showed a low spatial correlation between MNBN frequencies and $PM_{2.5}$ values. This result could be a direct consequence of Cerro de Hatonuevo geographic location on a hill-top up above the main coal mining areas. Pollutant dispersion mechanisms, depending both on the site topography and on the meteorological conditions strongly influence the concentrations of particles. It has been widely observed that for most airborne particulate and gas metrics, concentration reduces as wind speed increases, although in some cases, an increase in the concentration may be observed at the highest wind speeds (Jones et al., 2010). In consequence, as shown in Fig. 1, wind direction and speed around mining areas could disperse chemical substances from pits, storing and disposal sites and concentrate them around the flat areas of Chancletas, Provincial and San Francisco where predominant wind speed is reduced. This effect would be greatly enhanced by the mountainous area that borders these regions increasing the exposure. Besides low wind speed registered in Cerro de Hatonuevo, elevated topography in the area would also influence particles concentrations, increasing the deposition of PM_{10} and decreasing $PM_{2.5}$ levels. These results also demonstrate that geographical location of sampled areas and the associated relief also constitute a very important determinant of damage distribution and that must be considered in the analysis of health impact caused by dynamically distributed variables like the PM. In previous reports, we did not find a statistically significant association between PM_{10} levels and MNMONO frequency in exposed populations (Espitia-Perez et al., 2017). However, the spatial analysis showed a clustered relation between these variables at the south of the area of direct influence of the mining operations, as depicted in Fig. 3. Since exposed areas possess flat geomorphology, obtained results suggest that wind direction may also be related to spatial behavior rather than the localization of extraction zones. Prevailing wind would determine to a large extent the direction and deposition of a large portion of PM in the southern exposed areas, increasing the risk of elevated MNMONO frequencies in these populations. Even when the spatial relation was determined between MNMONO and PM_{10}, previous results about the $PM_{10}/PM_{2.5}$ ratio suggest that $PM_{2.5}$ constitutes a high proportion of PM_{10} in these areas (Espitia-Pérez, 2016); thus, the influence of $PM_{2.5}$ on MNMONO frequency must also be considered. On the other hand, considering that high deposition of PM_{10} occurs in areas near the emission source (Rojano et al., 2013; Huertas et al., 2014), it is also possible that some activities inside the pit and disposal sites could be producing high quantities of PM_{10}, also capable of inducing DNA damage (Roubicek et al., 2007; Jung et al., 2012). These results also demonstrate that geographical analyses of variables like PM and MN frequencies are capable of establishing correlations that commonly used statistical analysis may not.

Further analysis of other components of the PM also described interesting spatial correlations. Using inorganic elements concentrations previously obtained by PIXE analysis (Espitia-Perez et al., 2017), and consequently, EF values calculated for each element found in the $PM_{2.5}$ fraction, we established the presence of highly (S) and moderate enriched elements (Cr, Cu, Cl, and Zn) in coal mining areas. We employed EF values rather than element concentrations to evaluate the effects of anthropogenic sources of DNA

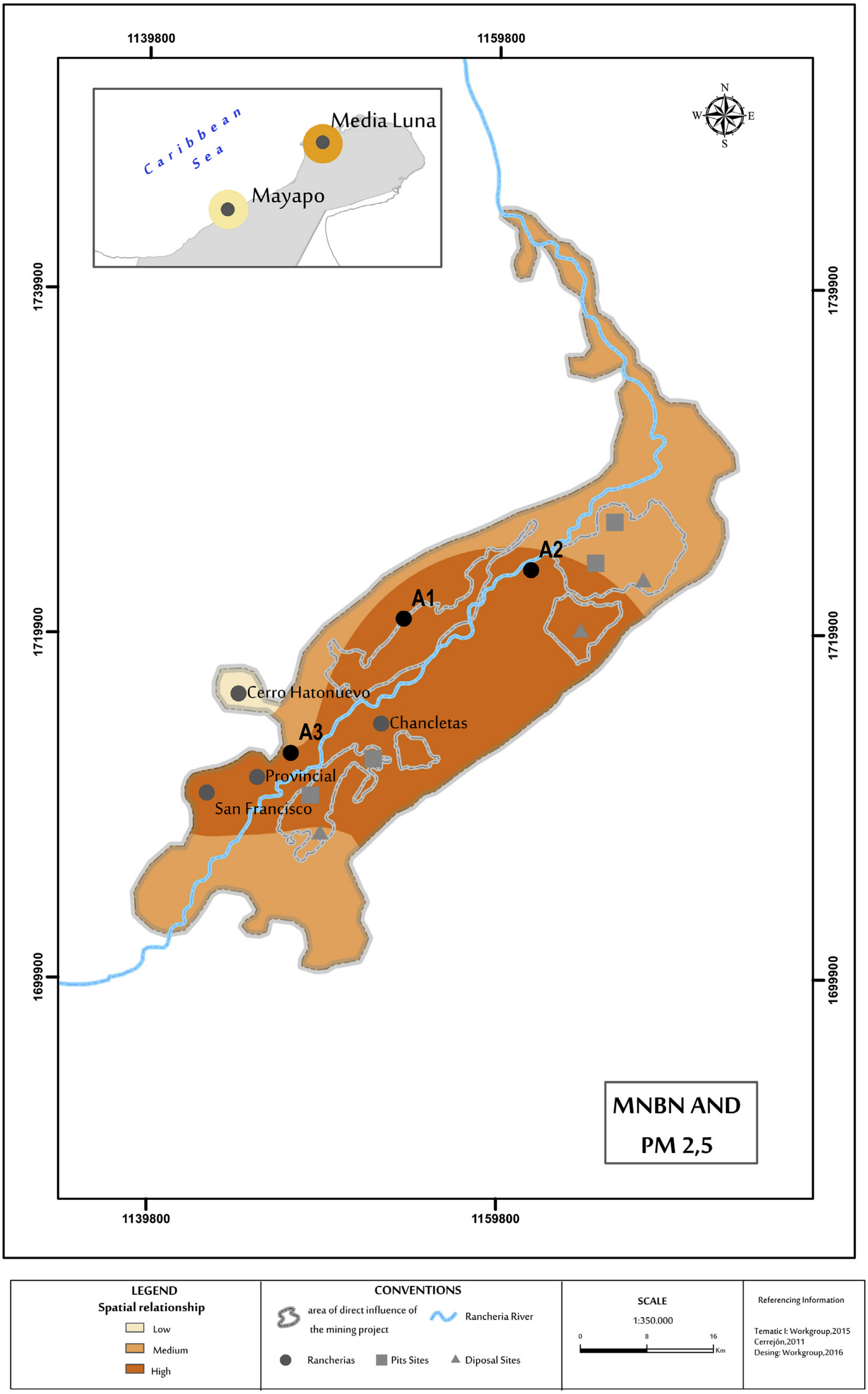

Fig. 2. Overlay analysis of MNBN frequency and $PM_{2.5}$ concentrations in areas located near the direct influence area of the open pit coal mining operations.

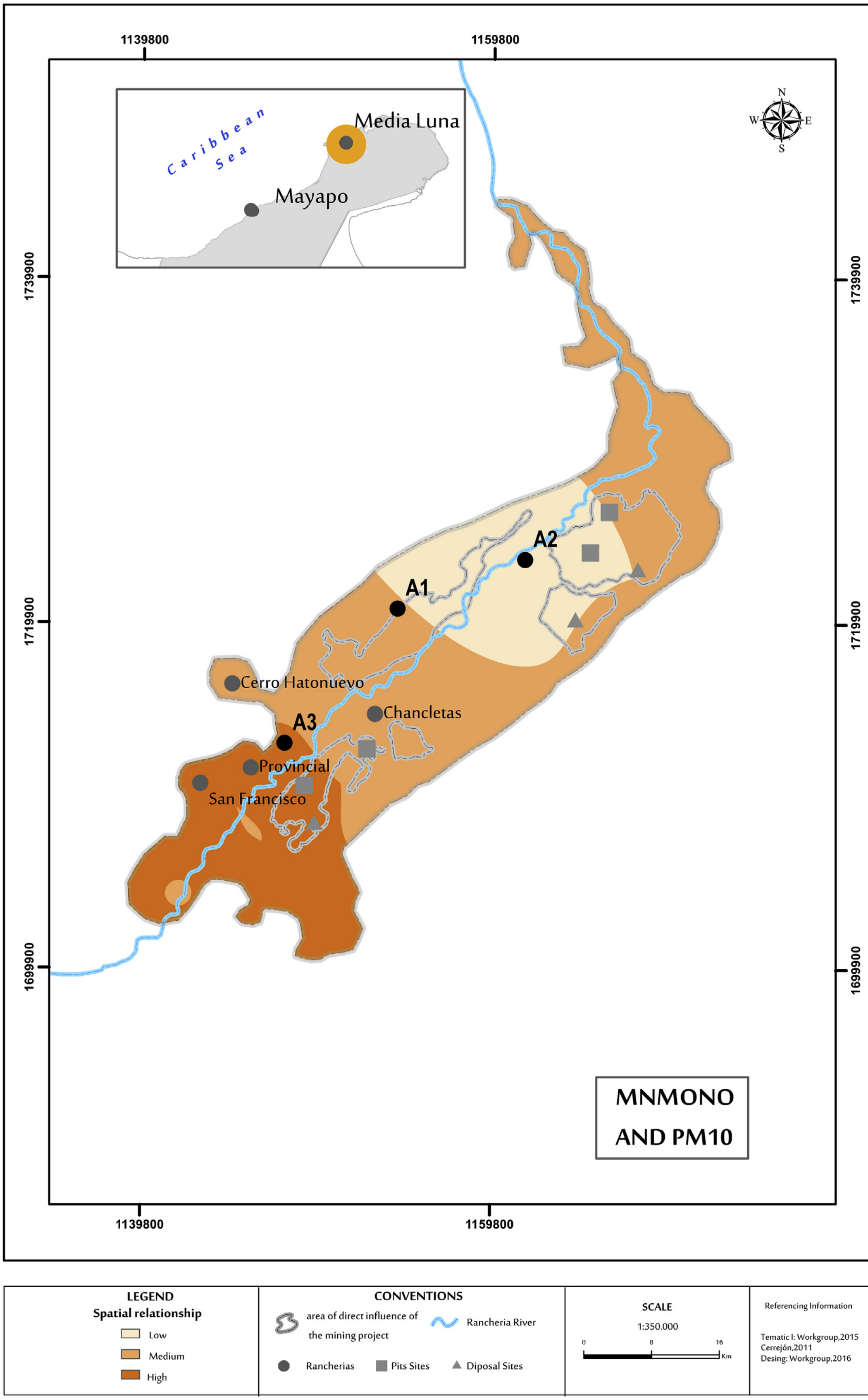

Fig. 3. Overlay analysis of MNMONO frequency and PM_{10} concentrations in areas located near the direct influence area of the open pit coal mining operations.

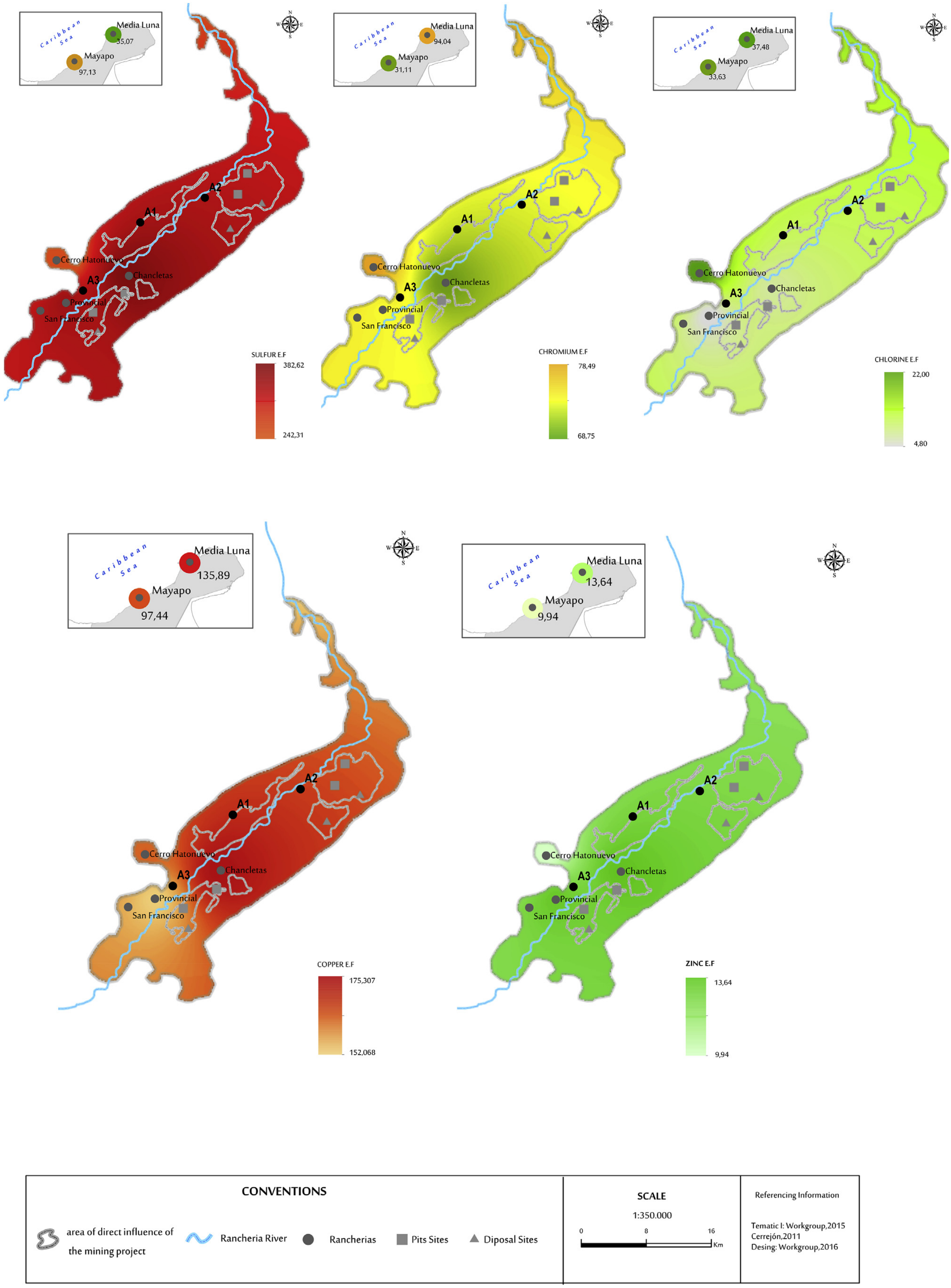

Fig. 4. Spatial EF distribution of S, Cr, Cl, Cu and Zn in sampling areas in proximity to the open pit coal mining operations.

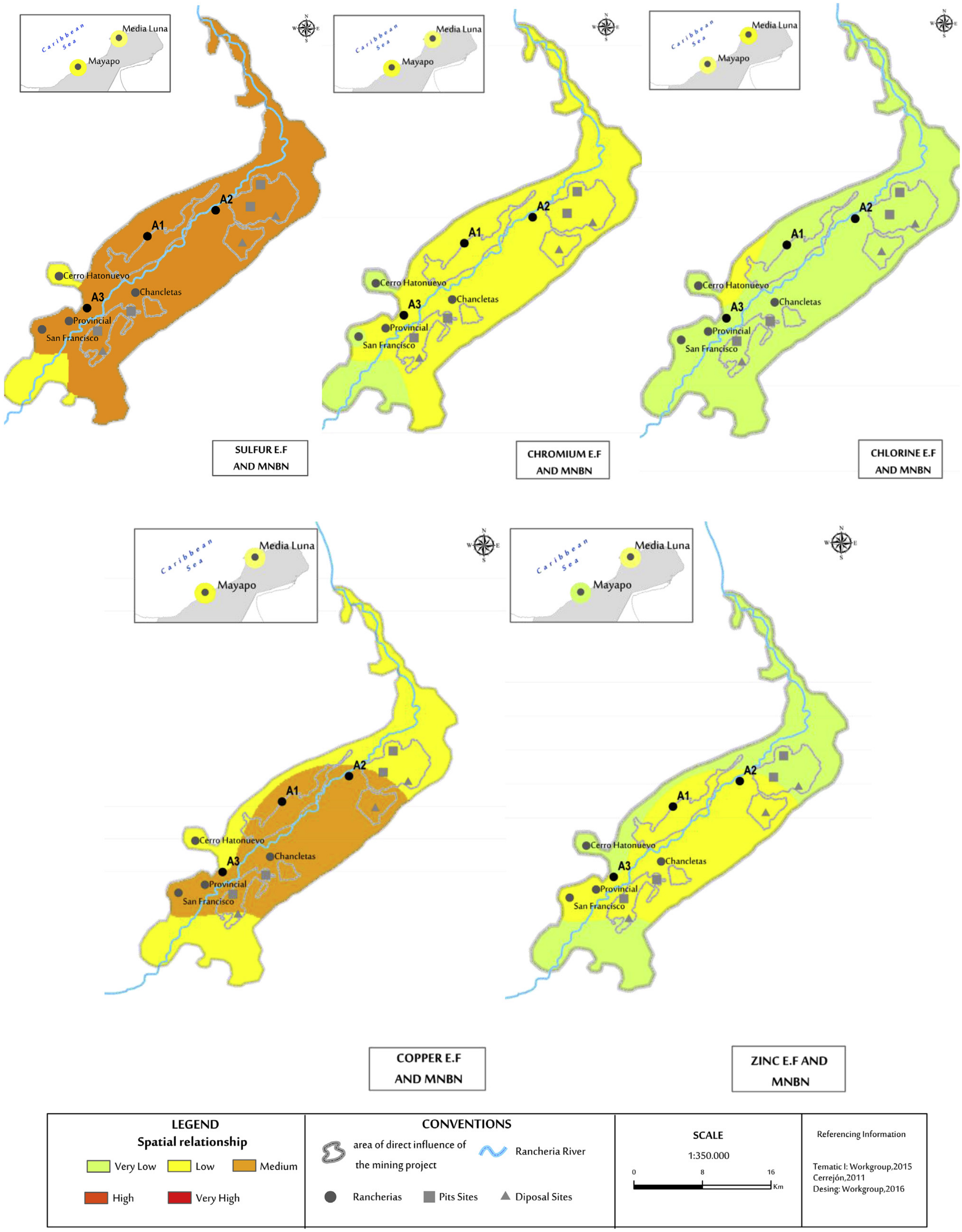

Fig. 5. Overlay analysis of interpolated MNBN frequencies and EF values of enriched elements in sampling areas in proximity to the open pit coal mining operations.

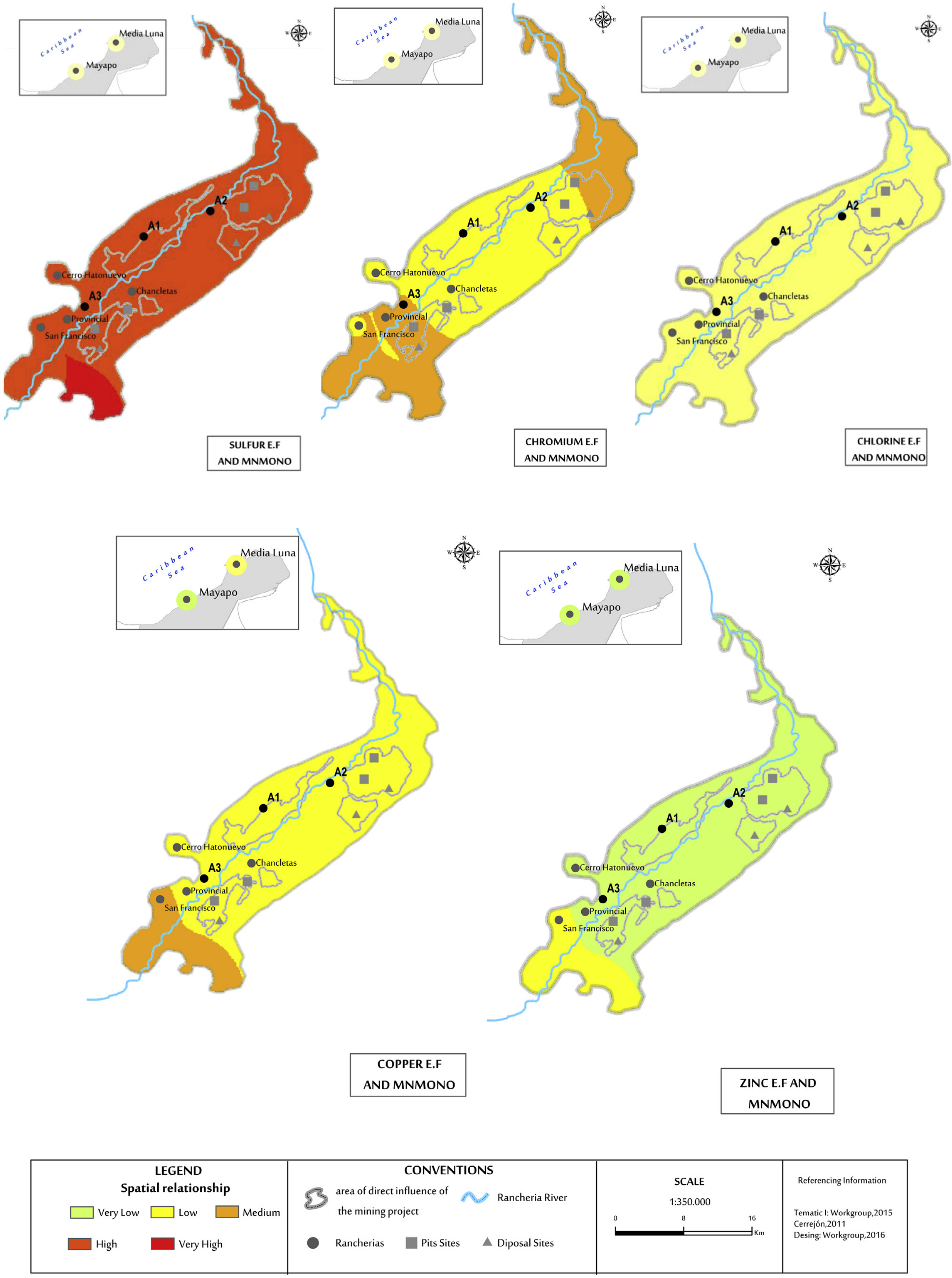

Fig. 6. Overlay analysis of interpolated MNMONO frequencies and enriched elements concentrations in sampling areas in proximity to the open pit coal mining operations.

damage, excluding possible interferences due to crustal elements contribution. We also wanted to corroborate if anthropogenic emission sources possessed any influence in the detected elemental EF and whether EF values and location of open-pits presented any spatial behavior. To locate the possible emission source responsible for high EF values in the sampling sites, we decided to perform an identification of pits, disposal and storing areas inside the mining areas. In a previous report by Rojano et al. (2016), were identified three areas for coal storage A1, A2, and A3. We only considered A1 and A3, as they were located near our sampling sites. However, residues from A2 may also be transported to sampled areas by the predominant wind. Fig. 4 shows the spatial distribution of EF values for S, Cr, Cu, Cl and Zn and possible emission sources around the coal mining area. Elements typically found around coal mining areas like S, Cu and Zn showed highly enriched patterns around pits and disposal sites, with a decrease of EF values with distance from the mining operations. Sulfur was highly enriched around storing piles A1 and A3, which could indicate that emissions are produced during coal mining and through active mine fires (Pandey et al., 2014). For S, emission sources may include S from common sulfide minerals contained in the coal, such as pyrite (Ward, 2008); thus, punctual emission sources of sulfur can be related as A1 in the north, A3 in the south and the Comuneros and Oreganal open-pits. These combustion residues could be dispersed by the wind along the whole mining area as shown in the interpolation results. The presence of S in sampled areas is a matter of concern since contributes to acid rain due to its responsibility in the production of sulfuric acid, responsible for the solubilization of metals in aerosol (Medunic et al., 2016) and especially in other ambient matrices, such as soil and water. Sulfate contamination of surface and groundwater from mining and processing operations is well recognized and commonly monitored as a primary indicator of coal mining impact to surface water (Simonton and King, 2013). Because several of the Wayúu and Afro-Colombians communities from the exposed areas use artesian wells in water supply, more future studies, focusing in analytical determination of S deposition in water samples are highly recommended around the coal mining influence zone. Analysis of the enrichment pattern for Cr showed higher values at north and south of the mining region, particularly around pits and disposal sites. Enrichment of Cr is a well-documented indication of their anthropogenic origin from traffic emissions (Kothai et al., 2009), especially caused by transporting operation of coal and coal mining sub-products around some areas inside the mining corridor. In line with this observation slightly elevated enrichment values of Cr were obtained around pits sites characterized by large-scale coal transportation using unpaved roads, as well as coal material overburden loading and unloading. Particularly in Media Luna, the presence of a coal railroad transportation may also be related to the EF found for Cr, commonly present in areas of increased trains activities (Cartledge and Majestic, 2015). The differential pattern obtained for the Cr enrichment values would suggest that dispersion of Cr from emission source might not be related to wind. Another element related to high vehicle traffic is Cu. However, in our results, the enrichment pattern was different from other traffic-related elements like Cr. Other possible sources of Cu enrichment in coal mines is related to coal fly ashes (Petaloti et al., 2006), that could be released by coal combustion in proximity to A3 and A1 storing piles. Similar results were obtained in an abandoned coal mine in Turkey (Yenilmez et al., 2011), in which Cu showed higher concentrations within the coal storage area and dumped sites. Similarly, high EF values for Zn may also be correlated with coal and coal bottom fly ash ((ATSDR), 2005). Similar distribution patterns observed for Cu and Zn seem to confirm a similar origin and distribution. Enrichment distribution pattern for Cl is possibly related to the presence of the water-soluble ion Cl from marine aerosol (Dao et al., 2014). In accordance with this assumption, EF values were lower around the coal mining area and higher in Mayapo and Media Luna both located near the coastal area. Higher concentrations of Cl around of Cerro de Hatonuevo coincide with the presence of clay soil with high salinity levels and brackish underground water zones.

Medium and low correlations between MNBN frequencies and S, Cr and Cu EF values around mining areas, would indicate that exposure to these enriched elements typically produced in coal mining activities, is in part related to increased MNBN frequencies. These observations would confirm previous observations (Espitia-Perez et al., 2017) showing that organic components of the $PM_{2.5}$ are very important for the effects on the cell cycle and DNA damage (Longhin et al., 2013). Interestingly, areas with higher EF values for S showed also higher frequencies of MNMONO cells, while other elements like Cr and Cu showed medium and low correlations. Except for Cu, Cl, and Zn, that seems to have similar correlations patterns, MNMONO frequencies apparently were more susceptible to the enrichment of S and Cr than MNBN. These results would indicate that enrichment of some elements like S and Cr around coal mining areas are potentially more related to accumulated in vivo genetic damage induction in exposed residents, which may also reflect an increase in the number of damaged cells that failed to divide. Some of these elements present in the $PM_{2.5}$ fraction are involved in the generation of oxidative damage through reactive oxygen species (ROS) production (Valko et al., 2006). As previously discussed, oxidative stress status inside the cell is capable of causing mitotic arrest (increasing MNMONO frequency), centromere damage, kinetochore malfunction (Parker et al., 2014) or disruption of the mitotic spindle (Choi et al., 2007) associated to aneugenic effects (Kraniak et al., 2006).

5. Conclusions

Results showed a spatial relationship between exposure to higher concentrations of $PM_{2.5}$ and PM_{10} and MN frequency in individuals with residential proximity to coal mining areas. Our study is one of the first attempts to perform a spatial analysis of the relationship between PM generation, proximity to coal mining areas and predictive cancer risk biomarkers in open-pit systems. Active pits, disposal, and storage areas could be identified as the possible sources of combustion elements associated with spontaneous coal seams fires. Wind speed and topography around the coal mining areas were identified as significant contributors to PM dispersion and damage distribution. The enrichment of the $PM_{2.5}$ fraction with inorganic elements contributes to the increase of MNBN frequencies of exposed populations and corroborates the main role of the organic components of the PM in the biological effects and DNA damage; however seems to be more related to increase MNMONO frequencies and DNA damage accumulated in vivo. The present study would pose a useful tool to assess the human health risk associated with residential proximity to open-pit coal mining areas and could help to supply detailed and hierarchical information to the public or government about detailed priority pollutants and regions of concern.

Acknowledgments

Authors gratefully wish to acknowledge the support of the national board of SINTRACARBON for logistic cooperation during the sampling period, to CORPOGUAJIRA and its evaluation, control and environmental monitoring group for the valuable technical and logistic assistance. We also thank the local Wayúu authorities from San Francisco, Media Luna, Cerro de Hatonuevo, Provincial and Mayapo and the Afro-Colombian leaders of Chancleta and Las

Casitas. This research was supported by COLCIENCIAS/Colombia (Grant no. 128356934353/2013), Universidad del Sinú/Colombia (UNISINU), Universidad del Cauca/Colombia (UNICAUCA), Universidad Luterana do Brasil (ULBRA), and Universidade Federal do Rio Grande do Sul/Brasil (UFRGS) through common research fund no. 751/2013.

Appendix A. Supplementary data

Supplementary data related to this article can be found at https://doi.org/10.1016/j.chemosphere.2018.04.049.

References

Agency for Toxic Substances and Disease Registry (ATSDR), 2005. Toxicological Profile for Zinc. U.S. Department of Health and Human Services, Public Health Service, Atlanta, GA.

Agudelo-Castañeda, D.M., Teixeira, E.C., Schneider, I.L., Lara, S.R., Silva, L.F.O., 2017. Exposure to polycyclic aromatic hydrocarbons in atmospheric PM1.0 of urban environments: carcinogenic and mutagenic respiratory health risk by age groups. Environ. Pollut. 224, 158–170.

Ahern, M., Hendryx, M., 2012. Cancer mortality rates in appalachian mountain top coal mining areas. J. Environ. Occup. Sci. 1, 63–70.

Annangi, B., Bonassi, S., Marcos, R., Hernandez, A., 2016. Biomonitoring of humans exposed to arsenic, chromium, nickel, vanadium, and complex mixtures of metals by using the micronucleus test in lymphocytes. Mutat. Res. 770, 140–161.

Azpurua, M.A., Ramos, K.D., 2010. A comparison of spatial interpolation methods for estimation of average electromagnetic field magnitude. Prog. Electromag. Res. M 14, 135–145.

Barja, B., Mogo, S., Cachorro, V.E., Antuña, J.C., Estevan, R., Rodrigues, A., de Frutos, Á., 2013. Atmospheric particulate matter levels, chemical composition and optical absorbing properties in Camagüey, Cuba. Environ. Sci. J. Integr. Environ. Res. Process. Impacts 15, 440–453.

Bhuiyan, M.A.H., Parvez, L., Islam, M.A., Dampare, S.B., Suzuki, S., 2010. Heavy metal pollution of coal mine-affected agricultural soils in the northern part of Bangladesh. J. Hazard Mater. 173, 384–392.

Bonassi, S., El-Zein, R., Bolognesi, C., Fenech, M., 2011. Micronuclei frequency in peripheral blood lymphocytes and cancer risk: evidence from human studies. Mutagenesis 26, 93–100.

Bonassi, S., Znaor, A., Ceppi, M., Lando, C., Chang, W.P., Holland, N., Kirsch-Volders, M., Zeiger, E., Ban, S., Barale, R., Bigatti, M.P., Bolognesi, C., Cebulska-Wasilewska, A., Fabianova, E., Fucic, A., Hagmar, L., Joksic, G., Martelli, A., Migliore, L., Mirkova, E., Scarfi, M.R., Zijno, A., Norppa, H., Fenech, M., 2007. An increased micronucleus frequency in peripheral blood lymphocytes predicts the risk of cancer in humans. Carcinogenesis 28, 625–631.

Calderon, J., Nieves, J., 2010. Informe calidad del aire corredor minero. In: Guajira, C.A.r.d.l. (Ed.), Corporación Autónoma. Corporación Autónoma regional de la Guajira.

Campagna, M., Pilia, I., Marcias, G., Frattolillo, A., Pili, S., Bernabei, M., d'Aloja, E., Cocco, P., Buonanno, G., 2017. Ultrafine particle distribution and chemical composition assessment during military operative trainings. Int. J. Environ. Res. Publ. Health 14.

Cao Guo Liang, Z.X., Gong, SunLing, An, Xin Qin, Wang, Ya Qiang, 2011. Emission inventories of primary particles and pollutant gases for China. Atmos. Sci. 56, 781–788.

Cartledge, B.T., Majestic, B.J., 2015. Metal concentrations and soluble iron speciation in fine particulate matter from light rail activity in the Denver-Metropolitan area. Atmos. Pollut. Res. 6, 495–502.

Cerrejón, S.A., 2011. Summary of the Iiwo'uyaa Expansion Project for Stakeholders, p. 70.

Choi, W.J., Banerjee, J., Falcone, T., Bena, J., Agarwal, A., Sharma, R.K., 2007. Oxidative stress and tumor necrosis factor-alpha-induced alterations in metaphase II mouse oocyte spindle structure. Fertil. Steril. 88, 1220–1231.

Colaizzi, G.J., 2004. Prevention, control and/or extinguishment of coal seam fires using cellular grout. Int. J. Coal Geol. 59, 75–81.

Dao, X., Wang, Z., Lv, Y., Teng, E., Zhang, L., Wang, C., 2014. Chemical characteristics of water-soluble ions in particulate matter in three metropolitan areas in the north China plain. PLoS One 9, e113831.

Dubey, B., Pal, A.K., Singh, G., 2012. Trace metal composition of airborne particulate matter in the coal mining and non–mining areas of Dhanbad Region, Jharkhand, India. Atmos. Pollut. Res. 3, 238–246.

EPA, U.S.E.P.A., 2006. 40 CFR Part 50. National Ambient Air Quality Standards for Particulate Matter; Final Rule EPA, U.S. (Environmental Protection Agency). Available online at:>. https://www3.epa.gov/ttnamti1/files/ambient/pm25/pt5006.pdf.

Espitia-Pérez, L., 2016. Efeitos biológicos do material particulado gerado em sistemas de mineração de carvão a céu aberto em populações humanas com exposição ambiental.

Espitia-Perez, L., da Silva, J., Espitia-Perez, P., Brango, H., Salcedo-Arteaga, S., Hoyos-Giraldo, L.S., de Souza, C.T., Dias, J.F., Agudelo-Castaneda, D., Valdes Toscano, A., Gomez-Perez, M., Henriques, J.A.P., 2017. Cytogenetic instability in populations with residential proximity to open-pit coal mine in Northern Colombia in relation to PM10 and PM2.5 levels. Ecotoxicol. Environ. Saf. 148, 453–466.

Espitia-Pérez, L., Sosa, M.Q., Salcedo-Arteaga, S., León-Mejía, G., Hoyos-Giraldo, L.S., Brango, H., Kvitko, K., da Silva, J., Henriques, J.A.P., 2016. Polymorphisms in metabolism and repair genes affects DNA damage caused by open-cast coal mining exposure. Mutat. Res. Genet. Toxicol. Environ. Mutagen 808, 38–51.

Fenech, M., 2006. Cytokinesis-block micronucleus assay evolves into a “cytome” assay of chromosomal instability, mitotic dysfunction and cell death. Mutat. Res. Fund Mol. Mech. Mutagen 600, 58–66.

Fenech, M., 2007. Cytokinesis-block micronucleus cytome assay. Nat. Protoc. 2, 1084–1104.

Ghose, M.K., Majee, S.R., 2007. Characteristics of hazardous airborne dust around an Indian surface coal mining area. Environ. Monit. Assess. 130, 17–25.

Hans Wedepohl, K., 1995. The composition of the continental crust. Geochem. Cosmochim. Acta 59, 1217–1232.

Hosgood, H.D., Chapman, R.S., Wei, H., He, X., Tian, L., Liu, L.Z., Lai, H., Engel, L.S., Chen, W., Rothman, N., 2012. Coal mining is associated with lung cancer risk in Xuanwei, China. Am. J. Ind. Med. 55, 5–10.

Huang, F., Pan, B., Wu, J., Chen, E., Chen, L., 2017. Relationship between exposure to PM2.5 and lung cancer incidence and mortality: a meta-analysis. Oncotarget 8, 43322–43331.

Huertas, J.I., Huertas, M.E., Cervantes, G., Díaz, J., 2014. Assessment of the natural sources of particulate matter on the opencast mines air quality. Sci. Total Environ. 493, 1047–1055.

Jenkins, W.D., Christian, W.J., Mueller, G., Robbins, K.T., 2013. Population cancer risks associated with coal mining: a systematic review. PLoS One 8, e71312.

Jha, D.K., Sabesan, M., Das, A., Vinithkumar, N., Kirubagaran, R., 2011. Evaluation of interpolation technique for air quality parameters in Port Blair, India. Univers. J. Environ. Res. Technol. 1, 301–310.

Jones, A.M., Harrison, R.M., Baker, J., 2010. The wind speed dependence of the concentrations of airborne particulate matter and NOx. Atmos. Environ. 44, 1682–1690.

Jung, M.H., Kim, H.R., Park, Y.J., Park, D.S., Chung, K.H., Oh, S.M., 2012. Genotoxic effects and oxidative stress induced by organic extracts of particulate matter (PM10) collected from a subway tunnel in Seoul, Korea. Mutat. Res. Genet. Toxicol. Environ. Mutagen 749, 39–47.

Kaonga, B., Kgabi, N.A., 2011. Investigation into presence of atmospheric particulate matter in Marikana, mining area in Rustenburg Town, South Africa. Environ. Monit. Assess. 178, 213–220.

Kirsch-Volders, M., Bonassi, S., Knasmueller, S., Holland, N., Bolognesi, C., Fenech, M.F., 2014. Commentary: critical questions, misconceptions and a road map for improving the use of the lymphocyte cytokinesis-block micronucleus assay for in vivo biomonitoring of human exposure to genotoxic chemicals-a HUMN project perspective. Mutation research. Rev. Mutat. Res. 759, 49–58.

Klimkina, I., 2013. Assessment of mutagenic health effects in coal mine workers. Genome 18, 31.

Kothai, P., Prathibha, P., Saradhi, I., Pandit, G., Puranik, V., 2009. Characterization of atmospheric particulate matter using PIXE technique. Int. J. Environ. Chem. Ecol. Geol. Geophys. Eng. 3, 38–42.

Kraniak, J.M., Abrams, J., Nowak, J.E., Tainsky, M.A., 2006. Antioxidant agents transiently inhibit aneuploidy progression in Li-Fraumeni cell strains. Mol. Carcinog. 45, 141–156.

Leon-Mejia, G., Espitia-Perez, L., Hoyos-Giraldo, L.S., Da Silva, J., Hartmann, A., Henriques, J.A., Quintana, M., 2011. Assessment of DNA damage in coal open-cast mining workers using the cytokinesis-blocked micronucleus test and the comet assay. Sci. Total Environ. 409, 686–691.

León-Mejía, G., Quintana, M., Debastiani, R., Dias, J., Espitia-Pérez, L., Hartmann, A., Henriques, J.A.P., Da Silva, J., 2014. Genetic damage in coal miners evaluated by buccal micronucleus cytome assay. Ecotoxicol. Environ. Saf. 107, 133–139.

Li, Q., Liu, H., Alattar, M., Jiang, S., Han, J., Ma, Y., Jiang, C., 2015. The preferential accumulation of heavy metals in different tissues following frequent respiratory exposure to PM2.5 in rats. Sci. Rep. 5, 16936.

Longhin, E., Holme, J.A., Gutzkow, K.B., Arlt, V.M., Kucab, J.E., Camatini, M., Gualtieri, M., 2013. Cell cycle alterations induced by urban PM2.5 in bronchial epithelial cells: characterization of the process and possible mechanisms involved. Part. Fibre Toxicol. 10, 1–19.

Medunic, G., Ahel, M., Mihalic, I.B., Srcek, V.G., Kopjar, N., Fiket, Z., Bituh, T., Mikac, I., 2016. Toxic airborne S, PAH, and trace element legacy of the superhigh-organic-sulphur Rasa coal combustion: cytotoxicity and genotoxicity assessment of soil and ash. Sci. Total Environ. 566–567, 306–319.

Melody, S.M., Johnston, F.H., 2015. Coal mine fires and human health: what do we know? Int. J. Coal Geol. 152 (Part B), 1–14.

Ministerio del Ambiente, 2017. Resolución No 2254 (Norma de calidad del Aire Ambiente), p. 11.

Nalder, I.A., Wein, R.W., 1998. Spatial interpolation of climatic normals: test of a new method in the Canadian boreal forest. Agric. For. Meteorol. 92, 211–225.

Pandey, B., Agrawal, M., Singh, S., 2014. Assessment of air pollution around coal mining area: emphasizing on spatial distributions, seasonal variations and heavy metals, using cluster and principal component analysis. Atmos. Pollut. Res. 5, 79–86.

Parker, A.L., Kavallaris, M., McCarroll, J.A., 2014. Microtubules and their role in cellular stress in cancer. Front. Oncol. 4, 153.

Patra, A.K., Gautam, S., Kumar, P., 2016. Emissions and human health impact of

particulate matter from surface mining operation—a review. Environ. Technol. Innovat. 5, 233–249.
Petaloti, C., Triantafyllou, A., Kouimtzis, T., Samara, C., 2006. Trace elements in atmospheric particulate matter over a coal burning power production area of western Macedonia, Greece. Chemosphere 65, 2233–2243.
Pone, J.D.N., Hein, K.A.A., Stracher, G.B., Annegarn, H.J., Finkleman, R.B., Blake, D.R., McCormack, J.K., Schroeder, P., 2007. The spontaneous combustion of coal and its by-products in the Witbank and Sasolburg coalfields of South Africa. Int. J. Coal Geol. 72, 124–140.
Ribeiro, J., da Silva, E.F., Flores, D., 2010. Burning of coal waste piles from Douro Coalfield (Portugal): petrological, geochemical and mineralogical characterization. Int. J. Coal Geol. 81, 359–372.
Rohr, P., Kvitko, K., da Silva, F.R., Menezes, A.P.S., Porto, C., Sarmento, M., Decker, N., Reyes, J.M., Allgayer, M.d.C., Furtado, T.C., Salvador, M., Branco, C., da Silva, J., 2013. Genetic and oxidative damage of peripheral blood lymphocytes in workers with occupational exposure to coal. Mutat. Res. Genet. Toxicol. Environ. Mutagen 758, 23–28.
Rojano, R., Angulo, L., Restrepo, G., 2015. Concentración y relación de PST, PM10 y PM2.5 en poblaciones cercanas a minería a cielo abierto: caso Cerrejón Colombia. Revista de la Facultad de Ingeniería U.C.V 30, 1–10.
Rojano, R., Arregocés, H., Angulo, L., Restrepo, G., 2016. PM10 emissions due to storage in coal piles in a mining industrial area. WIT Trans. Ecol. Environ. 207, 87–97.
Rojano, R.E., Angulo, L.C., Restrepo, G., 2013. Niveles de Partículas Suspendidas Totales (PST), PM10 y PM2.5 y su Relación en Lugares Públicos de la Ciudad Riohacha, Caribe Colombiano. Inf. Tecnol. 24, 37–46.
Roubicek, D.A., Gutiérrez-Castillo, M.E., Sordo, M., Cebrián-García, M.E., Ostrosky-Wegman, P., 2007. Micronuclei induced by airborne particulate matter from Mexico City. Mutat. Res. Genet. Toxicol. Environ. Mutagen 631, 9–15.
Simonton, D.S., King, S., 2013. Hydrogen sulfide formation and potential health consequences in coal mining regions. Water Qual. Expo. Health 5, 85–92.
Sun, L., Wu, Q., Liao, K., Yu, P., Cui, Q., Rui, Q., Wang, D., 2016. Contribution of heavy metals to toxicity of coal combustion related fine particulate matter (PM2.5) in Caenorhabditis elegans with wild-type or susceptible genetic background. Chemosphere 144, 2392–2400.
Taner, S., Pekey, B., Pekey, H., 2013. Fine particulate matter in the indoor air of barbeque restaurants: elemental compositions, sources and health risks. Sci. Total Environ. 454–455, 79–87.
Tchounwou, P.B., Yedjou, C.G., Patlolla, A.K., Sutton, D.J., 2012. Heavy metals toxicity and the environment. EXS 101, 133–164.
Valko, M., Rhodes, C.J., Moncol, J., Izakovic, M., Mazur, M., 2006. Free radicals, metals and antioxidants in oxidative stress-induced cancer. Chem. Biol. Interact. 160, 1–40.
Ward, I.C.L.a.C.R., 2008. Composition and mode of occurrence of mineral matter in some Colombian coals. Int. J. Coal Geol. 73, 3–18.
Wu, J., Winer, A.M., Delfino, J.R., 2006. Exposure assessment of particulate matter air pollution before, during, and after the 2003 Southern California wildfires. Atmos. Environ. 40, 3333–3348.
Yenilmez, F., Kuter, N., Emil, M.K., Aksoy, A., 2011. Evaluation of pollution levels at an abandoned coal mine site in Turkey with the aid of GIS. Int. J. Coal Geol. 86, 12–19.
Zandi, S., Ghobakhlou, A., Sallis, P., 2011. Evaluation of Spatial Interpolation Techniques for Mapping Soil PH.